J. Fluid Mech. (1972), *vol.* 53, *part* 1, *pp.* 177–191
Printed in Great Britain

A method for integrating the boundary-layer equations through a region of reverse flow

By J. B. KLEMP† AND ANDREAS ACRIVOS
Department of Chemical Engineering, Stanford University,
Stanford, California

(Received 19 July 1971)

If a region of reverse flow remains confined within a boundary layer the conventional boundary-layer equations should continue to apply downstream of the point of detachment of the surface streamline ($\Psi = 0$). Nevertheless, standard numerical techniques fail in the presence of backflow since these methods become highly unstable and, in addition, neglect the upstream flow of information. A procedure for numerically integrating the boundary-layer equations through a region of reverse flow which takes downstream influence into account is therefore presented. This method is then applied to the problem of uniform flow past a parallel flat plate of finite length whose surface has a constant velocity directed opposite to that of the main stream. Although singularities occur at both the point of detachment (x_s) and reattachment (x_r) of the $\Psi = 0$ streamline, this integration technique provides a solution which ceases to apply only in the close proximity of these singular points. From this solution it is evident that, throughout a large portion of the separated region, the flow is strongly affected by conditions near x_r, thereby demonstrating the importance of allowing information to be transmitted upstream in a region of backflow. Near x_s, however, it is found that, in spite of the presence of reverse flow, the solution has a self-similar form in this particular example.

1. Introduction

When a fluid flows past a solid body at high Reynolds number R, a thin viscous boundary layer is known to form at least along the forward portion of the solid surface. Under the influence of even a mild adverse pressure gradient, however, the motion within this boundary layer may be retarded to the extent that beyond a certain point x_s the direction of the flow near the surface becomes reversed. When this occurs, the forward moving fluid in the boundary layer detaches from the surface at x_s, being deflected away from the wall by a region of backflow which forms downstream. This phenomenon is commonly known as separation.

In most theoretical analyses of steady flows at high Reynolds number the complications arising because of the presence of boundary-layer separation are severe. If the surface streamline ($\Psi = 0$) downstream of x_s is displaced an order one distance from the body, the structure of the entire flow field is altered from that which would exist in the absence of separation, since fluid in the free stream

† Present address: National Center for Atmospheric Research, Boulder, Colorado.

now flows past an effective body whose surface contour differs significantly from that of the solid object. Even the boundary layer forming upstream of the point of detachment is affected, through its dependence on the pressure distribution in the adjacent main stream. Consequently, when the region of reverse flow is $O(1)$ in thickness, the analysis of the flow field is generally prohibitively difficult because the flow both in the main stream and in the separated region strongly depends on the position of the $\Psi = 0$ streamline downstream of x_s, which is *a priori* unknown.

If, on the other hand, the dividing streamline beyond its point of detachment is displaced a distance $\phi(x; R)$ from the body such that $O(R^{-\frac{1}{2}}) \leqslant \phi(x; R) < O(1)$, the problem is somewhat simplified owing to the fact that $\phi \to 0$ as $R \to \infty$. As a result, the first approximation to the solution in the main stream is not influenced by the separated region which exists downstream of x_s. Furthermore, the first-order boundary-layer solution upstream of x_s (except perhaps very near x_s) is also independent of ϕ since the governing equations depend, to this order, only on the $O(1)$ pressure gradient along the surface, as calculated, in the usual manner, from the potential flow. It remains then to determine the flow structure between the surface of the body and the detached portion of the $\Psi = 0$ streamline. An example of this type is the uniform flow past a flat plate with surface injection, in which, as shown recently by Kassoy (1971) and by Klemp & Acrivos (1972), the $\Psi = 0$ streamline is displaced a distance of $O(R^{-\frac{1}{3}})$ from the plate.

A further simplification results, however, when $\phi(x; R)$ is $O(R^{-\frac{1}{2}})$ since in this case the boundary-layer equations should remain valid both upstream and downstream of x_s except, possibly, in the immediate neighbourhood of this point. Nevertheless, fundamental difficulties are still encountered when a solution to these equations is sought downstream of x_s because standard methods of numerical integration yield solutions which depend, at any point in the flow field, only on conditions upstream. In the region of backflow, however, information is clearly being transferred upstream; hence the solution in a rather sizeable portion of the separated region may be significantly affected by the nature of the flow downstream. Since conventional integration procedures do not allow the flow to be affected by any downstream conditions, it should be expected that these methods, in addition to being highly unstable when reverse flow occurs, would also prove to be quite inaccurate.

In considering a problem for which $\phi(x; R) = O(R^{-\frac{1}{2}})$ downstream of x_s, Catherall & Mangler (1966) obtained a numerical solution to the boundary-layer equations beyond the point of detachment of the $\Psi = 0$ streamline. Although, in their scheme, the equations were integrated in a conventional manner well upstream of the separation point, their numerical technique was altered as x_s was approached in order to allow the solution to take into account the small change in pressure due to the presence of the separated region. This was accomplished by specifying the displacement thickness of the boundary layer, leaving the pressure distribution to be determined from the calculations. By following this procedure, Catherall & Mangler found that the boundary-layer equations could be integrated in a forward direction through a region of reverse flow and that the solution remained regular in the vicinity of x_s.

Catherall & Mangler's solution is a significant achievement in that it provides, apparently, the first successful integration of the boundary-layer equations past the point of separation. Nevertheless, it is not evident that their procedure represents a general approach to the problem because, in all physical applications, it is the shape of the solid boundary rather than the displacement thickness which is given. In addition, since the thickness of the separated region remains $O(R^{-\frac{1}{2}})$, the pressure distribution resulting from the appearance of this region is similarly $O(R^{-\frac{1}{2}})$ in magnitude and, as remarked earlier, this small pressure effect should disappear from the first-order boundary-layer equations as $R \to \infty$. Consequently, if the pressure distribution is uniquely determined from the surface contour as $R \to \infty$, Catherall & Mangler's method may only serve to create a body shape for which the separated region will remain $O(R^{-\frac{1}{2}})$ in width by forcing the solution to produce a specified $O(R^{-\frac{1}{2}})$ profile for the displacement thickness. Besides, the fact that the boundary-layer equations were integrated in a forward direction through the region of backflow raises further doubts regarding their technique.

In the present paper, we propose a method of solution for problems where $\phi(x; R)$ remains $O(R^{-\frac{1}{2}})$ beyond x_s, using an approach, quite different from Catherall & Mangler's, which does not suffer from the limitations discussed above. First, we take it for granted that the boundary-layer equations describe the viscous flow near the wall both upstream and downstream of the point of detachment, and that the pressure distribution at the edge of the boundary layer is determined from the potential-flow solution, which neglects the small displacement thickness of this viscous region. We then show that solutions to the boundary-layer equations can be obtained numerically (except possibly very near the points of detachment and reattachment) provided that the downstream influence arising from the presence of reverse flow is properly taken into account.

In a recent article, Briley (1971) used the full Navier–Stokes equations to solve for the flow in the vicinity of a separation bubble which remains inside the boundary layer downstream of x_s. However, since, in his solutions, at large but finite Reynolds numbers the streamwise velocity gradients appear to remain $O(1)$ in magnitude, there is strong indication that in the limit $R \to \infty$ his equations would reduce, in effect, to the conventional boundary-layer equations everywhere except possibly very near x_s. Although Briley argued that owing to their parabolic nature these equations cannot take downstream influence into account, we shall presently demonstrate that quite the opposite is true in a region of reverse flow.

In what follows, we shall not be concerned with the detailed structure of the boundary-layer solution at the point of separation x_s or the point of reattachment x_r. Rather, the object here will be to provide a method for integrating the boundary-layer equations through a region of backflow which allows information to be transmitted in the direction of the flow throughout the separated region. Of course, in applying this method to a particular problem it should become evident whether a singularity exists at x_s or x_r, although, even if this does happen, the boundary-layer solution should still remain valid except in a small neighbourhood of these singular points.

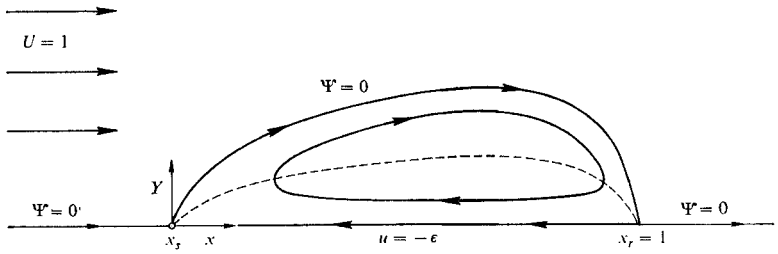

FIGURE 1. Uniform flow past a finite flat plate with surface velocity $-\epsilon$. ---, $u = 0$, $Y = \Gamma(x)$.

The specific problem to be considered here concerns the uniform flow at high R past a parallel flat plate of finite length which, although stationary, has its surface moving at a constant dimensionless velocity $-\epsilon$ in a direction opposite to that of the uniform stream. As shown in figure 1, the flow as $R \to \infty$ contains a recirculating region which forms within the boundary-layer adjacent to the moving surface of the plate. This basic structure was suggested by Leal & Acrivos (1969), who, through numerical solutions to the full Navier–Stokes equations for $R \leqslant 80$, showed that when ϵ is small both the width of the separation bubble and the displacement thickness of the viscous region become very small as R becomes large. Before solving this specific example, however, we shall first describe in § 2 a general procedure for numerically integrating the boundary-layer equations in a region of reverse flow which takes into account the influence of conditions downstream; we shall then apply this numerical technique, in § 3, to the solution of the finite plate problem mentioned above.

It will become evident from the resulting computations that near the trailing edge of the plate the solution is strongly affected by conditions near the point of reattachment. In the vicinity of x_s, however, the influence of the trailing edge is small, and consequently the flow pattern in the forward portion of the separated region is of a similar form to that for a semi-infinite plate. This similarity solution has some interesting features of its own which will be described in § 4. There, it will be shown that no boundary-layer solutions of this type can exist for $\epsilon > 0{\cdot}3541$ and that a seemingly peculiar behaviour of the shear stress profile is, in fact, physically realistic.

Although the flow problem to be discussed does not involve separation due to the action of an adverse pressure gradient, it will be shown in § 2 that the method of solution also applies to problems involving a non-zero longitudinal pressure profile. Moreover, it is felt that the present numerical procedure represents a realistic approach to these more conventional separation problems, provided that the displacement thickness remains $O(R^{-\frac{1}{2}})$ downstream of x_s.

2. Method of integration

We shall describe here a technique for integrating the boundary-layer equations through a region of reverse flow, deferring until § 3 the application of this integration procedure to a specific problem. We begin with the familiar

boundary-layer equations in their dimensionless form:

$$u\frac{\partial u}{\partial x}+V\frac{\partial u}{\partial Y}=-\frac{dp}{dx}+\frac{\partial^2 u}{\partial Y^2}, \quad \frac{\partial u}{\partial x}+\frac{\partial V}{\partial Y}=0, \tag{2.1}$$

where Y is the stretched co-ordinate normal to the surface, V is the normal velocity multiplied by $\sqrt{R}$, and the remaining variables have their usual meaning (Rosenhead 1963). Also, the pressure profile $p(x)$ is assumed known from the potential-flow solution evaluated at the surface of the body. Anticipating the specific problem to be considered in § 3, we require that $u(x, 0) = u_0(x)$ which, of course, reduces to the conventional no-slip condition if $u_0(x) \equiv 0$. The boundary conditions for (2.1) then become

$$\left.\begin{aligned} u = u_0(x), \quad V = 0 \quad \text{at} \quad Y = 0, \\ u = U(x) \quad \text{as} \quad Y \to \infty, \end{aligned}\right\} \tag{2.2}$$

along with an appropriate initial condition at $x = 0$. Here, $U(x)$ denotes the fluid speed at the edge of the boundary layer and is related to $p(x)$ by Bernoulli's equation.

We next suppose that (2.1) and (2.2) will continue to apply beyond x_s provided that the thickness of the separated region remains $O(R^{-\frac{1}{2}})$ downstream of the point of boundary-layer detachment. However, since standard numerical techniques fail whenever reverse flow occurs, it is necessary to devise a different procedure for the integration of these well-known equations. Specifically, the method to be presented here will take proper account of the downstream conditions by requiring that the direction of integration should coincide with the direction of flow. To this end, we divide the flow field into two regions denoted by I and II respectively, where I represents the region of reverse flow near the surface while II corresponds to the remaining portion of the flow domain where $u > 0$. Along the line $Y = \Gamma(x)$, separating I and II, $u = 0$ and $V = V_0(x)$, both $\Gamma(x)$ and $V_0(x)$ being, at first, unknown. It should be noted that $V_0(x)$ will be positive in the forward portion of the recirculating region and negative towards the rear. The original problem thus separates into two separate boundary-layer problems in I and II which, as will be shown, can be solved in each region by integrating the equations in the appropriate direction of the flow.

For purposes of this analysis it is more convenient to rewrite (2.1) using Prandtl's transposition theorem (Rosenhead 1963, p. 211), which yields

$$u\frac{\partial u}{\partial x}+v\frac{\partial u}{\partial \zeta}=-\frac{dp}{dx}+\frac{\partial^2 u}{\partial \zeta^2}, \quad \frac{\partial u}{\partial x}+\frac{\partial v}{\partial \zeta}=0, \tag{2.3}$$

where

$$\zeta \equiv Y - \Gamma(x)$$

and

$$v(x, \zeta) = V(x, \zeta) - \Gamma'(x)\, u(x, \zeta),$$

$\Gamma'(x)$ denoting the x derivative of Γ. The boundary conditions for each region are then

$$\left.\begin{aligned} u = u_0(x), \quad v = -\Gamma'(x)\, u_0(x) \quad \text{at} \quad \zeta = -\Gamma(x), \\ u = 0 \quad \text{at} \quad \zeta = 0, \end{aligned}\right\} \quad \text{in region I,} \tag{2.4}$$

$$\left.\begin{aligned} u = 0, \quad v = V_0(x) \quad &\text{at} \quad \zeta = 0, \\ u = U(x) \quad &\text{at} \quad \zeta \to \infty, \end{aligned}\right\} \quad \text{in region II.} \tag{2.5}$$

Hence, the boundary-layer problem is as shown in figure 2, where x_r denotes the reattachment point of reverse flow region.

Clearly, since $\Gamma(x)$ and $V_0(x)$ are initially unknown it is necessary to set up an iterative procedure for obtaining the correct solutions in regions I and II. To begin with, we assume a profile for $\Gamma(x)$ and then solve the boundary-layer problem in I, proceeding in the negative x direction from x_r forward to x_s. This is possible because after having specified $\Gamma(x)$ we are left, in view of (2.4), with a properly posed problem for region I; hence, (2.3) can be solved numerically using standard techniques for the integration of nonlinear parabolic differential equations. Note that initial conditions are not required for this step since the width of I is reduced to a point at x_r. Also, in constructing the finite-difference scheme we determine the solution at any point A in I from the three adjacent points, as shown in figure 2. As a result, information is now transmitted upstream, in the direction of flow. This integration yields, then, the flow pattern in I plus the function $V_0(x)$.

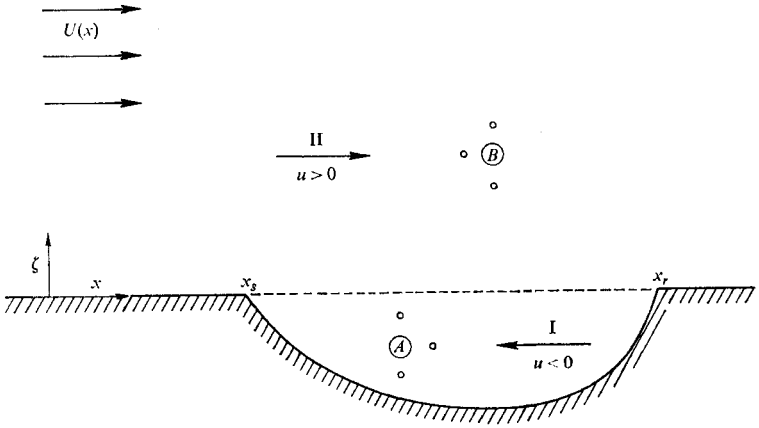

FIGURE 2. Boundary-layer problem in the transformed co-ordinates. ---, $u = 0$, $v = V_0(x)$; ▨, $\zeta = -\Gamma(x)$, $u = u_0(x)$, $v = -\Gamma'(x)u_0(x)$.

Turning next to the region of forward flow, one integrates (2.3) subject to (2.5), proceeding step by step in the downstream direction. Since the solution upstream of x_s is independent of the flow in I, this integration may begin at x_s for each iteration, after the flow upstream has been evaluated. The solution at a point B in the flow field is determined from the neighbouring points as shown in figure 2, so that, again, information is transferred in the direction of the fluid motion. This completes one full iteration.

To determine if the correct profile for $\Gamma(x)$ was chosen initially, we next compute the shear stress at $\zeta = 0$, the boundary between the two regions. Clearly, this shear stress should be continuous; otherwise, a new function $\Gamma(x)$ must be selected and the iteration procedure repeated. Note that, since integration of the boundary-layer equations has been carried out in both regions I and II using

well-established integration techniques, the corresponding shear stress profiles at $\zeta = 0$ can be computed for a given $\Gamma(x)$ without difficulty. Therefore, the procedure should converge provided a better approximation for $\Gamma(x)$ can be selected following each iteration. Although it may not be clear initially how to alter $\Gamma(x)$ at each step, a method will be described in § 3 for accomplishing this in connexion with the particular problem being discussed there.

This integration scheme should yield a solution valid throughout the separated region provided the boundary-layer equations do not become singular at either x_s or x_r. However, even if singularities do arise at x_s and x_r, it would appear that, using this integration technique, a solution could still be obtained which would cease to apply only locally, in the close proximity of these two points. In the following section, we shall return to this subject of singularities and demonstrate that the present numerical scheme is successful in spite of the appearance of singularities.

In order to check the results of the above integration scheme and provide an alternative procedure for treating boundary layers containing reverse flow, a second method was developed for solving (2.1) directly. However, because this approach does not appear to be as successful in the presence of singularities as the procedure described above, it will be described only briefly here. In this scheme, integration of the boundary-layer equations proceeds throughout the flow field in the downstream direction. At each value of x, the finite-difference formulation for the associated column of points is constructed so that the solution at each point depends on its neighbours in the manner indicated by B in figure 2, when $u > 0$, and by A when $u < 0$. Thus the portion of a column in the region of reverse flow is influenced by points downstream while the remainder of the column makes use of upstream information in the usual way. Of course, by means of this procedure of integrating column by column through the separated region, it is only possible, after each pass, to transfer information across a single column upstream. For this reason, one must continue to sweep through the boundary layer, beginning each pass at x_s, until the solution ceases to vary, within prescribed limits, at each point in the flow. Although a few solutions for the problem in § 3 were obtained using this method and agreed well with those generated by the other technique, difficulties were sometimes encountered near x_s and x_r, indicating that this integration scheme tends to become unstable in the vicinity of singular points. As a result, in what follows we shall refer only to the first method described above.

3. Solution for a finite flat plate with negative surface velocity

To illustrate an application of our numerical technique we consider here the uniform flow of an incompressible fluid at high Reynolds number R past a parallel flat plate of finite length whose surface moves with a constant velocity in a direction opposite to that of the main stream. For the purposes of this analysis, the variables are rendered dimensionless in the usual manner by using the plate length l and the velocity U' of the uniform stream, hence $R \equiv U'l/\nu$, where ν is the kinematic viscosity of the fluid. Also, the constant velocity of the plate surface

is denoted by $-\epsilon$. The co-ordinate system is defined in figure 1, which also depicts the basic structure of the flow.

Following the suggestion of Leal & Acrivos (1969), we begin by assuming, subject to *a posteriori* verification, that the separated region becomes $O(R^{-\frac{1}{2}})$ in thickness as $R \to \infty$, provided that ϵ is small. Thus, in the ensuing analysis we shall retain the standard boundary-layer equations but omit the pressure gradient term, since the velocity becomes uniform at the outer edge of the viscous layer. Of course, in the present special case the region of reverse flow results from the negative surface velocity of the plate. In addition, we note that this backflow is confined to a region directly above the surface of the plate, as indicated in figure 1. This result is suggested by the findings of Leal & Acrivos (1969), based on the numerical solutions of the full Navier–Stokes equations for $R \leqslant 80$, and can be justified in the following manner. Let us suppose that the separation bubble did in fact extend upstream of the leading edge of the plate. Then, since the boundary-layer equations are parabolic, an infinite velocity gradient would exist on the upstream side of the detached $\Psi = 0$ streamline in the proximity of x_s and the net effect of this would be to drive x_s back to the leading edge. On the other hand, if the bubble extended downstream of the trailing edge the boundary-layer equations would have only a trivial solution in the region of reverse flow for $x > 1$, since the boundary conditions there would become $\partial u/\partial Y = V = 0$ at $Y = 0$ and $u = 0$ at $Y = \Gamma(x)$. This point regarding the location of reattachment was further verified by solving the equations using the second procedure described in the previous section in which it is not necessary to specify *a priori* the value of x_r. Thus, in this particular case, x_s will coincide with the leading edge at the origin and x_r will be located at the trailing edge, $x = 1$.

In this problem, the boundary-layer equations become singular at both x_s and x_r, owing to the discontinuity in the boundary conditions. Because x_s is at the leading edge, however, this singularity can be removed from the equations by expressing them in terms of a set of new independent variables in a manner analogous to that frequently used for obtaining solutions near the leading edge of conventional boundary-layer problems. Thus, putting

$$\Psi(x,\eta) = (x/R)^{\frac{1}{2}} f(x,\eta), \quad \eta = \zeta/x^{\frac{1}{2}} = [Y - \Gamma(x)]/x^{\frac{1}{2}} \tag{3.1}$$

and substituting into (2.1), we obtain, in place of (2.3),

$$2f_{\eta\eta\eta} + f f_{\eta\eta} = 2x[f_\eta f_{x\eta} - f_x f_{\eta\eta}], \tag{3.2}$$

with the boundary conditions

$$f_\eta = -\epsilon, \quad f_x = -\epsilon[\Gamma'(x) - \Gamma(x)/2x]/x^{\frac{1}{2}} \quad \text{at} \quad \eta = -x^{-\frac{1}{2}}\Gamma(x), \quad (0 \leqslant x \leqslant 1),$$

$$f_\eta = 0 \quad \text{at} \quad \eta = 0,$$

and

$$f_\eta = 1 \quad \text{at} \quad \eta \to \infty.$$

Note that as $x \to 0$ the right-hand side of (3.2) vanishes. Hence, near $x = 0$, (3.2) admits a similarity solution with $\Gamma \sim x^{\frac{1}{2}}$ which corresponds to that of the uniform flow past a semi-infinite plate with negative surface velocity. This result seems

reasonable since we would expect conditions near the trailing edge of the plate to have little effect on the flow near the origin. The similarity solution has some rather interesting features which will be discussed briefly in § 4, where it will be demonstrated that boundary-layer solutions having this similar form can exist only for $\epsilon \leqslant 0{\cdot}3541$. Thus, for the problem of a finite plate the technique described above will only lead to a solution provided that $\epsilon \leqslant 0{\cdot}3541$. On the other hand, if ϵ exceeds this critical value it is not evident that the boundary-layer approximations remain valid in the limit $R \to \infty$.

With this in mind, we now follow the integration procedure outlined in the previous section which begins by dividing the flow field into two regions separated by the line $u = 0$. Since this curve corresponds to $\eta = 0$, the boundary conditions for the integration of (3.2) become

$$\left.\begin{aligned} f_\eta = -\epsilon, \quad f_x = -\epsilon[\Gamma'(x) - \Gamma(x)/2x]/x^{\frac{1}{2}} \quad &\text{at} \quad \eta = -x^{-\frac{1}{2}}\Gamma(x), \\ f_\eta = 0 \quad &\text{at} \quad \eta = 0, \end{aligned}\right\} \quad \begin{matrix}\text{in region I} \\ (u < 0),\end{matrix} \tag{3.3}$$

$$\left.\begin{aligned} f_\eta = 0, \quad f = f(x, 0) \quad &\text{at} \quad \eta = 0, \\ f_\eta = 1 \quad &\text{as} \quad \eta \to \infty, \end{aligned}\right\} \quad \text{in region II} \quad (u > 0), \tag{3.4}$$

where $f(x, 0)$, corresponding to $V_0(x)$ in § 2, is initially unknown. The boundary-layer equations can then be integrated according to the prescribed method. For each iteration, (3.2) is first integrated in I subject to (3.3); when $f(x, 0)$ has been determined, the boundary conditions in (3.4) are used to integrate (3.2) through region II. After each iteration the new profile for $\Gamma(x)$ is generated from the relation

$$\Gamma_{i+1}(x) = \Gamma_i(x)\left\{1 + r\,\frac{\frac{\partial u_{\mathrm{I}}}{\partial \eta}(x, 0^-) - \frac{\partial u_{\mathrm{II}}}{\partial \eta}(x, 0^+)}{\frac{\partial u_{\mathrm{II}}}{\partial \eta}(x, 0^+)}\right\}, \tag{3.5}$$

in which r is a relaxation parameter whose values lie in the range $0 < r \leqslant 1$. Note that if the shear stress at $\eta = 0^+$ is greater than that at $\eta = 0^-$, (3.5) will decrease $\Gamma(x)$ for the next iteration, thereby causing the gradients in I to become larger, and *vice versa*. Although there is no guarantee that the profile for $\Gamma(x)$ will remain smooth after a number of iterations, no such difficulties were encountered in the present case provided that r was suitably chosen. For example, for very small values of ϵ, r could be set equal to 1, while as ϵ approached the critical value of $0{\cdot}3541$, r had to be reduced to about $0{\cdot}3$. Of course, the task of determining $\Gamma(x)$ is simplified to some extent in the present problem by the fact that the position of x_r is known. However, even if this were not the case, it does not appear that the iteration procedure would become significantly more difficult. In particular, by choosing initially a profile for $\Gamma(x)$ which extends beyond the true point of reattachment it should be possible to generate the correct curve by means of the above iteration process, with $\Gamma(x)$ being driven to zero at each point downstream of x_r.

As was mentioned in the previous section, this integration scheme should converge if accurate approximations to $\Gamma(x)$ can be chosen in successive iterations. In the problem considered here, convergent solutions were obtained using

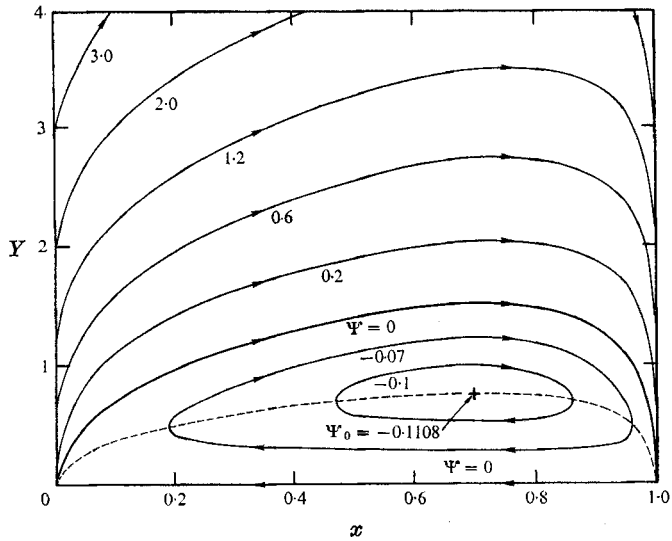

FIGURE 3. Structure of the flow field for $\epsilon = 0{\cdot}3$ (values of the stream function have been multiplied by $R^{\frac{1}{2}}$). ---, $u = 0$; +, vortex centre.

(3.5) which, it would appear, should remain successful for other problems of this type. However, even if (3.5) were to prove inadequate for some particular case, one should still be able to use the present procedure provided that (3.5) could be replaced with a more appropriate criterion for altering $\Gamma(x)$ after computing the shear stress profiles at $\zeta = 0^{\pm}$.

Although the singularity at x_s was removed from the equations by using (3.1), a similar transformation could not be found for dealing with the trailing-edge singularity of the boundary-layer equations. Nevertheless, the presence of this singularity at x_r did not seem to influence the stability of the integration scheme. Rather, owing to the breakdown of the boundary-layer equations, it only appeared to affect the accuracy of the solution near x_r which, of course, could be improved by employing a small mesh size near the trailing edge. For this reason, in integrating (3.2) in I and II the mesh size dx in the streamwise direction was continually decreased as x_r was approached. Thus, for the numerical results to be presented, dx was varied from 0·0025 near $x = 1$ to about 0·08 near the origin, where deviations from the similarity solution are small. The transverse mesh size $d\eta$ was set at 0·04 in all cases. In this manner, solutions were generated for a number of values of ϵ in the range $0 < \epsilon \leqslant 0{\cdot}35$. A typical streamline pattern for the flow field is plotted in figure 3 for $\epsilon = 0{\cdot}3$.

To illustrate how the structure of the separated region depends on ϵ, we have plotted in figure 4 the position of the $\Psi = 0$ streamline for $\epsilon = 0{\cdot}1$, 0·2 and 0·3. For purposes of comparison, we have also included the corresponding curves for the semi-infinite plate, which were calculated from the similarity solution mentioned earlier. Clearly, for $\epsilon = 0{\cdot}1$ the finite plate solution deviates from that of the semi-infinite case only in the close vicinity of x_r. In contrast, when ϵ is increased to 0·3 the two solutions coincide only for a short distance downstream of x_s. Thus, it is evident that as ϵ becomes larger the existence of reattachment at

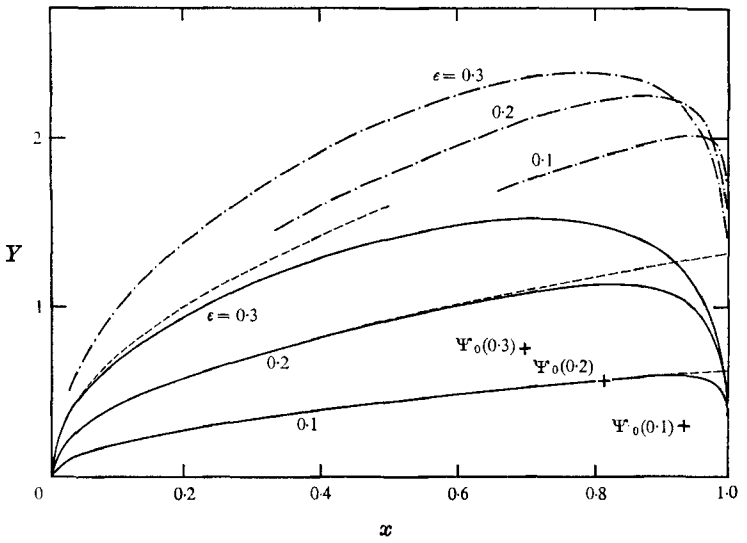

FIGURE 4. Structure of the separated flow region as a function of ϵ. ——, $\Psi = 0$ streamline; – – –, $\Psi = 0$ streamline based on the similarity solution; —·—·, displacement thickness; +, vortex centre with minimum stream function, $\Psi_0(\epsilon)$. $\Psi_0(0{\cdot}3) = -0{\cdot}1108$, $\Psi_0(0{\cdot}2) = -0{\cdot}0522$, $\Psi_0(0{\cdot}1) = -0{\cdot}0146$.

the trailing edge plays an increasingly significant role throughout the separated region.

Other interesting features of the flow are also depicted in figure 4. From the indicated positions of the vortex centres, we find that for each ϵ this point is located at the same value of x, where the bubble has its maximum width, and that it gradually moves upstream with increasing ϵ. In addition, the height of the vortex centre is only slightly less than half the maximum height of the corresponding $\Psi = 0$ line, both of these being proportional to ϵ when ϵ is small. Although it has not been plotted here, the shape of $u = 0$ line is similar to that of the dividing streamline, its Y co-ordinate for a given x being about half that of the latter. Finally, we have included in figure 4 the displacement-thickness curves for these values of ϵ. It can be seen that, whereas the width of the separation bubble increases approximately in proportion to ϵ, the displacement thickness shifts outward more slowly.

The increasing deviation of the finite plate solution from the similarity form is further evidenced in the surface shear stress profiles plotted in figure 5. Note here that the region of large shear stress associated with the singularity at x_s extends further and further upstream as ϵ is increased. Thus, the drag coefficient first decreases with increasing ϵ, as the similarity solution will be seen to indicate, and then begins to increase as a result of the rise in the shear stress along the rear portion of the plate. Specifically, the drag coefficient was found to decrease from 0·664 at $\epsilon = 0$ to a minimum of 0·633 at about $\epsilon = 0{\cdot}25$, before beginning to increase. Although it may seem peculiar that the drag coefficient should first decrease as the surface velocity becomes more negative, we shall demonstrate in the next section that this behaviour is quite realistic.

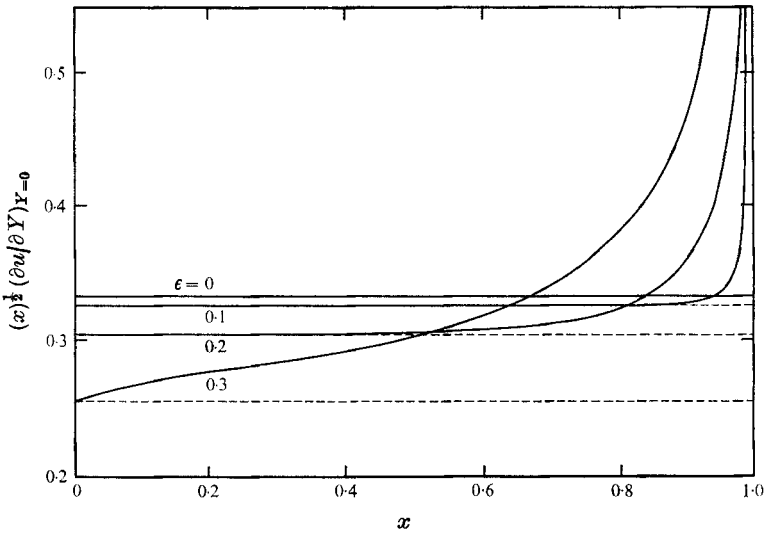

FIGURE 5. Surface shear stress profiles for various ϵ.
——, finite plate; – – –, similarity solution.

From these solutions it is clear that conditions near the point of reattachment of the dividing streamline can strongly affect the flow in upstream portions of the separated region. In addition, profiles for the displacement thickness show that in spite of singularities which may arise at x_s and x_r the boundary-layer thickness can remain $O(R^{-\frac{1}{2}})$ throughout the region of backflow, provided that ϵ is not too large. When this happens, the procedures outlined in § 2 seem to provide a useful method for integrating the boundary-layer equations, even in the presence of these singularities. In fact, the finite plate problem was also solved without using the transformation given in (3.1). In this instance, the solution was again obtained without difficulty, although, as expected, it was found to be somewhat more inaccurate over the forward portion of the bubble.

Admittedly, the problem discussed in this section differs in many important respects from one involving separation due to an adverse pressure gradient. Nevertheless, it appears that by successfully applying the integration procedure to the above example we have been able to demonstrate that the present method is entirely capable of dealing with a class of problems in which a region of reverse flow is contained within a boundary layer.

4. Discussion of the similarity solution

It is evident from the results of the previous section that, in the upstream portion of the separated region, the solution has a similar form which can be obtained by solving (3.2) with the right-hand side set equal to zero. Here, we shall discuss some of the interesting features of this solution. To begin with, we note that the transformation given by (3.1) is no longer required since by expressing the stream function in the similar form

$$\Psi(x, \eta') = (x/R)^{\frac{1}{2}} f(\eta'), \quad \eta' = Y/x^{\frac{1}{2}} \tag{4.1}$$

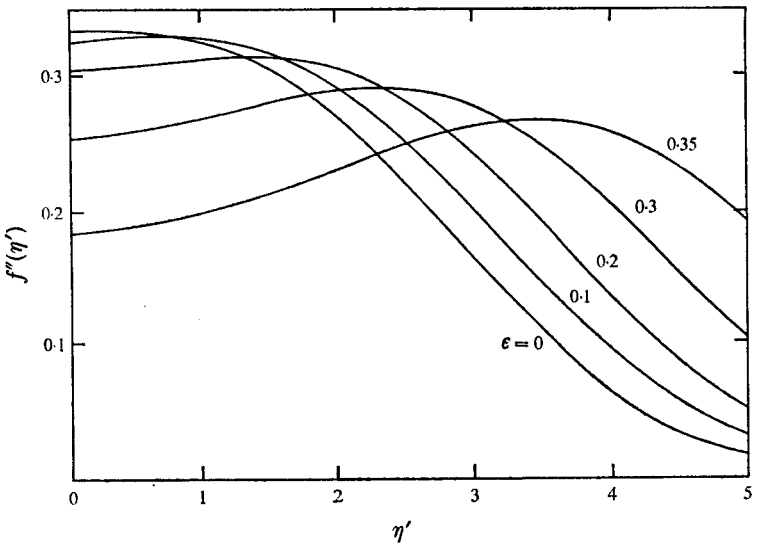

FIGURE 6. Shear stress profiles from the similarity solution for various ϵ.

it is possible to reduce the boundary-layer equations simply to the familiar Blasius equation

$$2f''' + ff'' = 0 \tag{4.2}$$

with boundary conditions

$$f(0) = 0, \quad f'(0) = -\epsilon, \quad f'(\infty) = 1.$$

The solution for $f(\eta')$, which can be obtained readily through the numerical integration of (4.2), represents, then, the solution for the problem of uniform flow past a semi-infinite flat plate with a negative surface velocity relative to the free stream equal to $-\epsilon$. It is found that, although, as expected, $f'(\eta')$ increases monotonically from $-\epsilon$ to unity with increasing η', the profiles for $f''(\eta')$, being proportional to the shear stress, have a more unusual shape, as shown in figure 6. Notice that when ϵ is positive (corresponding to a negative surface velocity) the shear stress reaches a maximum in the interior of the flow field, and that as ϵ is increased the surface shear stress decreases. These same results were obtained by Leal & Acrivos (1969)† who then concluded that this solution was physically unacceptable owing to the unrealistic form of the shear stress profile. However, we shall now demonstrate that this similarity solution is, in fact, the correct solution for a semi-infinite plate with a negative surface velocity, provided that $\epsilon \leqslant 0{\cdot}3541$, and that the observed shear stress profile, rather than being unrealistic, is actually what should be expected.

To understand the significance of this solution better, let us examine its form in the region where $f'(\eta') > 0$, which lies above the $u = 0$ line given by $Y = \Gamma(x)$. Recalling that the solution must be independent of the length scale chosen, we

† Other investigators have also computed solutions to (4.2) but have not commented on their behaviour for $\epsilon > 0$ (see Robillard 1971).

require that $\Gamma(x) = Cx^{\frac{1}{2}}$, where C is a positive constant. Thus, by using the transformation (3.1), which replaces $f(x, \eta)$ by $F(\eta)$, we obtain

$$\left.\begin{aligned} 2F''' + FF'' &= 0, \\ F(0) = f(C), \quad F'(0) &= 0, \quad F'(\infty) = 1, \end{aligned}\right\} \tag{4.3}$$

which is identical to the similarity problem describing the uniform flow past a parallel flat plate with a surface injection velocity given by $v_0(x) = -f(C)/2(Rx)^{\frac{1}{2}}$. Here, $f(C)$ is determined from the solution of (4.2) at the point where $f'(\eta') = 0$.

Solutions to (4.3) have been tabulated by Emmons & Leigh (1954) for $f(C) > -1{\cdot}2386$ and illustrate the well-known fact that as the blowing velocity is increased the wall shear stress decreases, and that the region of large shear stress is displaced into the interior of the boundary layer. Consequently, the interpretation of the solution to (4.2) is clear: the main stream flowing past the plate sees a no-slip surface at $Y = \Gamma(x)$ through which fluid, supplied from downstream by the reverse flow in the region $0 < Y < \Gamma(x)$, is blown into the forward moving stream with velocity $v_0(x)$. This vertical flow then acts to decrease the surface shear stress and to displace the shear stress maximum away from the wall in the same manner as in the injection problem given by (4.3). As ϵ is increased $f(C)$ becomes more negative, corresponding to a larger blowing velocity.

Of course, for the blowing problem described by (4.3), conventional boundary-layer theory ceases to apply when $f(C) \leqslant -1{\cdot}2386$, since the boundary layer is then 'blown away' from the plate (Kassoy 1971; Klemp & Acrivos 1972). For this reason, it might be expected that the solution to (4.2) would no longer exist when ϵ is increased to the point where $f(C)$ equals this critical value. In actual fact, it was found that solutions to (4.2) could not be obtained if $\epsilon > 0{\cdot}3541$, corresponding to $f(C) = -0{\cdot}3812$, which is substantially larger than $-1{\cdot}2386$, the critical value for 'blow-off'. In addition, although, as indicated in figure 6, the wall shear stress decreases rapidly as $\epsilon \to 0{\cdot}3541$, $f''(0)$ is still quite positive at this critical point and, in fact, equals $0{\cdot}1557$. Moreover, when ϵ was increased by 10^{-4}, the numerical solution was observed to drift slowly until $f'(\eta') = -0{\cdot}3542$ throughout the flow field, indicating that at this value of ϵ the thickness of the region of reverse flow becomes thicker than $O(R^{-\frac{1}{2}})$. Thus, although it is clear that for $\epsilon > 0{\cdot}3541$ the strength of the reverse flow is such that the boundary-layer approximations cease to apply, it is not apparent at present why this should occur at that particular value of ϵ.

Finally, it should be remarked that in arriving at this similarity solution we have not really neglected the downstream influence on the flow. This is because, owing to the absence of a characteristic length in the case of a semi-infinite plate, the solution, if it exists, must be self-similar in order to remain independent of whatever length scale l is chosen. Consequently, both upstream and downstream effects on the solution at any point in the flow must be such that the similar form is maintained. On the other hand, as shown in the previous section, if the plate is finite in length, this similarity solution is valid only in the forward portion of the separated region since the existence of reattachment at the trailing edge of the plate influences the solution upstream of x_r.

This work was supported in part by grants NSF GK-4062 and NASA-NgR-05-020-420 and by a N.A.S.A. Traineeship to J. B. K.

REFERENCES

BRILEY, W. R. 1971 A numerical study of laminar separation bubbles using the Navier–Stokes equations. *J. Fluid Mech.* **47**, 713.

CATHERALL, D. & MANGLER, K. W. 1966 Integration of the two-dimensional laminar boundary-layer equations past the point of vanishing skin friction. *J. Fluid Mech.* **26**, 163.

EMMONS, E. W. & LEIGH, D. C. 1954 Tabulation of the Blasius function with blowing and suction. *Aero. Res. Counc. Current Paper*, no. 157.

KASSOY, D. R. 1971 On laminar boundary-layer blow-off. Part 2. *J. Fluid Mech.* **48**, 209.

KLEMP, J. B. & ACRIVOS, A. 1972 High Reynolds number flow past a flat plate with strong blowing. *J. Fluid Mech.* **51**, 337.

LEAL, L. G. & ACRIVOS, A. 1969 Structure of steady closed streamline flows within a boundary layer. *Phys. Fluids*, **2** (suppl.), 105.

ROBILLARD, L. 1971 On a series solution for the laminar boundary layer on a moving wall. *Trans. A.S.M.E.* E **38**, 550.

ROSENHEAD, L. (ed.) 1963 *Laminar Boundary Layers*. Oxford University Press.